Fundamentals and practice of metal contacts to wide band gap semiconductor devices

M. A. Borysiewicz*[1], E. Kamińska[1], M. Myśliwiec[1], M. Wzorek[1], A. Kuchuk[1,2], A. Barcz[1,3], E. Dynowska[1,3], M.-A. di Forte-Poisson[4], C. Giesen[5], and A. Piotrowska[1]

[1] Institute of Electron Technology, Al. Lotnikow 32/46, 02-668 Warsaw, Poland
[2] V. E. Lashkaryov Institute of Semiconductor Physics, 41 pr. Nauki, Kyiv, Ukraine
[3] Institute of Physic PAS, Al. Lotnikow 32/46, 02-668 Warsaw, Poland
[4] Alcatel-Thales III-V Lab, Route de Nozay, 91461 Marcoussis cedex, France
[5] AIXTRON SE, Kaiserstr. 98, 52134 Herzogenrath, Germany

Presented are the theoretical and experimental fundamentals of the fabrication of ohmic contacts to n- and p-type wide band gap semiconductors such as SiC and GaN. In particular, the Ni-Si/n-SiC, Al-Ti/p-SiC, Ti-Al/n-GaN and Ni-Au/p-GaN systems are discussed with the focus on the thermally activated chemical reactions taking place at the metal-semiconductor interface, that lead to the appearance of ohmic behaviour in the contact. Examples of reactions at very intimate interfaces are shown, which are irresolvable using even such sophisticated characterisation methods as high-resolution transmission electron microscopy and can only be explained using modelling. The issue of thermal stability of the contacts is discussed and the introduction of specifically designed diffusion barriers (eg. Ta-Si-N) into the contact metallisation stack is presented as a solution improving drastically the thermal stability of the contacts without degrading their electrical properties.

1 Introduction

There is considerable and stable growth of the need for electronic devices operating in high power and high frequency conditions and also for ones that would exhibit material and performance stability at high temperatures and in reducing atmospheres. Such devices find wide applications in the wireless communications RF field developing rapidly due to the massive increase in the number and performance of personal portable devices and on the other hand in the demand from specialised users, such as military and sat-communications for RF devices, that would operate in extreme environments. Another factor impacting the demand is the development of environmental sustainability and the so-called green power solutions where novel devices used for energy generation, distribution and conversion are needed. A final example of an industrial sector consuming a high number of devices working in harsh environments would be the automotive industry.

The intrinsic properties of wide band gap semiconductors (high breakdown fields, high electron saturation drift velocities, good thermal conductivity and resistance to oxidation) make them key materials for applications in such devices. SiC power devices are already on the market, and this material is also considered as good substrate material for high power high frequency GaN-based devices due to the very high thermal conductivity of SiC. On the other hand, GaN structures already find applications in commercial low to mid power high frequency devices. SiC is also an extensively studied substrate for large area graphene growth for application in transistors, with a graphene FET with a cut-off frequency equal to 100 GHz recently demonstrated by IBM [1].

---

* Corresponding author: e-mail: mbory@ite.waw.pl

However, although SiC and GaN exhibit high stability as discussed above, the complete device is also composed of elements such as ohmic contacts and Schottky barriers which not only have to provide high performance (low specific contact resistivity in the case of ohmic contacts and large barrier height in the case of Schottky contacts), but also maintain this performance in the harsh working conditions of the device. Therefore, the aim of this work is not only to summarise the basics of ohmic contact formation to n- and p-type SiC and GaN through the explanation of the relevant chemical reactions both in the contact metallisation as well as on the metal-semiconductor interface, but also to discuss the issue of the thermal and chemical stability of the formed ohmic contacts and potential measures that may be used to improve it.

2   Principles of ohmic contact formation

An ohmic contact is a metal-semiconductor junction which is characterized by current flow through it at variable bias which obeys Ohm's law. Such contacts, alongside the Schottky barrier contacts are needed in all electronic devices for precise and predictable current control and reliable device behavior. In general, a metal-semiconductor junction will be characterized by a finite potential barrier forming at the interface between the two materials. The height of the barrier is usually a complex function of the metal work function, the electron affinity of the semiconductor and the density and energy of the surface states of the semiconductor. In order to obtain an ohmic junction, the current flow through the barrier has to be achieved with as low energy as possible, in other words, the barrier has to be an easy obstacle to overcome. This can be generally realized in many ways, the two most significant of which are: (1) a lowering of the barrier to enable the carriers to overcome it only due to the thermal energy of the system kT, or (2) a thinning of the barrier in order to enable quantum mechanical carrier tunneling through the barrier. The barrier engineering can be done before and after the formation of the metal-semiconductor junction. In the former, one may dope the semiconductor in the subcontact region using ion implantation in order to fabricate a highly doped region that would thin the depletion region after the formation of the metal-semiconductor junction and thus thin the barrier itself and allow current tunneling through it. Another way to achieve this is to generate an intermediate semiconductor layer at the surface of the starting semiconductor through deposition. In order to lower the height of the barrier, the deposition of a complex metallisation may lead do the formation of such metal-semiconductor alloys after annealing, that will have lowered barrier height with respect to the starting metallisation stack. Furthermore, interfacial reactions with the semiconductor can lead to a further lowering or thinning of the barrier through reactions at a very intimate interface or an outdiffusion of carriers from the semiconductor, respectively. The thermally activated metal-semiconductor reactions will be the topic of this article.

3   Ohmic contacts to SiC

The technology of forming an ohmic metal-SiC contact consists of the deposition of an appropriate metallic stack and subsequent annealing. The annealing leads to the formation of metallic alloys between the metals and in some cases also between the metals and the substrate. As we will show there are also interfacial reactions that can play a decisive role in the formation of the ohmic contact. The thermally activated reactions between metals and SiC can be divided into two categories of metals taking place in two temperature ranges: (1) for metals such as eg. Ni, Pd and Pt, the products of the reaction, which takes place at around 350-450 °C, are silicides (Ni_xSi_y, Pd_xSi_y, PtSi) and carbon and (2) for refractory metals, such as Ti, Zr or W, the products of the reaction, which takes place at around 650-850 °C, are carbides (TiC, ZrC, WC) and silicon. We will now show the application of both of these reaction groups for contacts to n and p-type SiC.

3.1   Ni-Si based ohmic contacts to n-SiC   It is long known from the mature silicon technology, that thin Ni films deposited onto n-Si form a low-resistivity contact [2]. With the development of SiC-based technology Ni was also chosen for the ohmic metallization to n-SiC as it again forms a low-resistivity contact [3]. The problem however is, that the annealing needed for ohmic contact formation in such a Ni-SiC junction (see figure 1) destroys the smooth interface between the metal and semiconductor through the alloying of Ni with Si (see figure 2) into Ni_2Si.
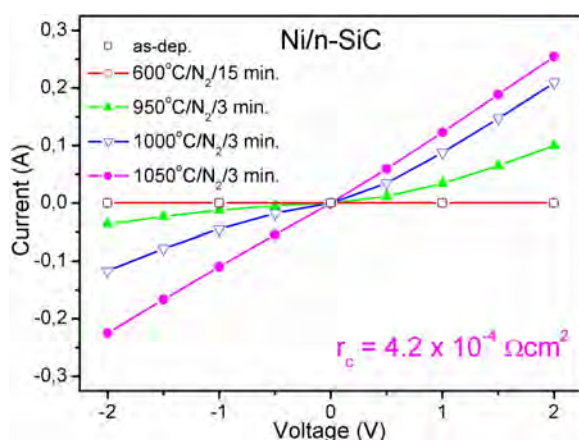

Fig. 1 I-V characteristics of a 100 nm Ni/n-SiC contact as deposited and when annealed under a nitrogen flow. After heat treatment at 1050 °C for 3 min ohmic contacts with specific contact resistance $r_c = 4.2 \times 10^{-4}$ $\Omega \cdot cm^2$ were achieved for SiC doped to $n = 2 \times 10^{17}$ cm^{-3}.
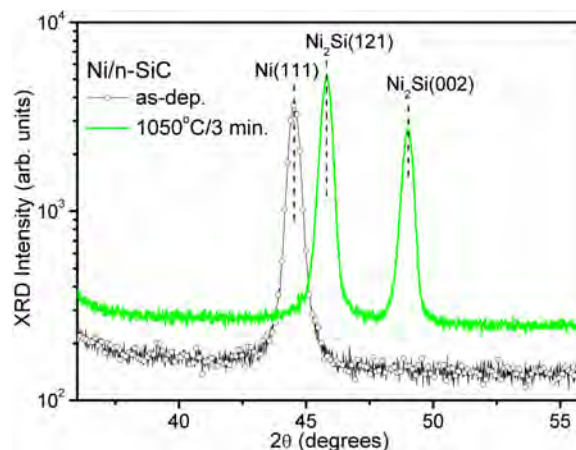
Fig. 2 X-ray diffraction pattern the 100 nm Ni/n-SiC contact measured after deposition and after the heat treatment providing ohmic behavior.

Therefore we decided to study and optimize the contact formation by an experiment in which instead of depositing single Ni films, a deposition of Ni and Si multilayers was performed, which would supply enough Si to Ni for an Ni-Si alloy to form, without removing the Si from the substrate [4,5]. We adjusted the thicknesses of the Ni and Si films in such a way, that the Ni:Si ratio in the deposited stack is in correspondence with either the Ni_2Si or $NiSi_2$ stoichiometry to determine which of these two phases determines ohmic contact formation. This, combined with using Ni or Si as the film contacting the substrate, yielded a total of four combinations, named 'Ni-Si-A' through 'Ni-Si-D', which are summarized in table 1.

Table 1 Samples prepared for the investigations of Ni/Si-based junctions to SiC.

Sample name	Ni thickness (nm)	Si thickness (nm)	Film order, substrate at left
'Ni-Si-A'	33.10	30.30	Si/Ni/Si/Ni
'Ni-Si-B'	33.10	30.30	Ni/ Si/Ni/Si/Ni
'Ni-Si-C'	13.75	50.50	Si/Ni/Si/Ni
'Ni-Si-D'	13.75	101.00	Ni/Si/Ni

The samples discussed here were prepared using DC magnetron sputtering of nickel and silicon onto n-4H-SiC substrates that were not intentionally heated during deposition. The carrier concentration in the substrates was equal to 2×10^{17} cm^{-3}. Circular transmission line method (c-TLM) patterns for the characterization of metal-semiconductor contact behavior were prepared using photolithography and lift-off technique. Post-deposition annealing was preformed in an RTP furnace under nitrogen flow. A first low-temperature 15 min long stage at 600 °C was used to enable good intermixing within the deposited layers without etching of the substrate. Subsequent 3 min long high temperature annealings were performed to discover the ohmic contact formation temperature. The temperatures used at this stage were between 800 °C and 1100 °C raised with a step of 50 °C. The structure of the obtained layers was investigated using X-ray diffraction (XRD), Rutherford backscattering (RBS) depth profiling and transmission electron microscopy (TEM) cross section imaging with electron diffraction measurements.

Figures 3 and 4 show the I-V characteristics measured for the 'Ni-Si-A' and 'Ni-Si-C' samples, respectively. The characteristics for the samples 'Ni-Si-B' and 'Ni-Si-D' have the same character and were not shown for brevity. Ohmic I-V behavior is observed only for the 'Ni-Si-A' sample with the stack stoichiometry of Ni_2Si after annealing at 1000 °C and higher. The measured specific contact resistivities are equal to 4.0×10^{-4} $\Omega \cdot cm^2$, 3.5×10^{-4} $\Omega \cdot cm^2$ and 5.0×10^{-4} $\Omega \cdot cm^2$ for annealing at 1000 °C, 1050 °C and 1100 °C, respectively. The specific contact resistivity at 1050 °C for the sample 'Ni-Si-B' with the Ni layer at the

interface was equal to $5.5 \times 10^{-4} \, \Omega \cdot cm^2$ and the contact became non-ohmic after annealing at 1100 °C, which shows, that it is important to deposit the Si layer as the first one.
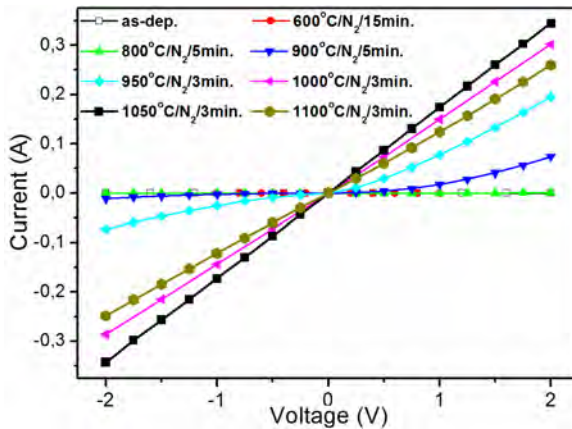

Fig. 3 I-V characteristics measured for a Ni/Si/Ni/Si/n-SiC structure as deposited and after subsequent annealing steps at 600 °C, and then from 900 °C to 1100 °C with a step of 50 °C. The thicknesses of the Ni and Si films were equal to 33.1 nm and 30.3 nm, respectively (sample 'Ni-Si-A' from table 1).
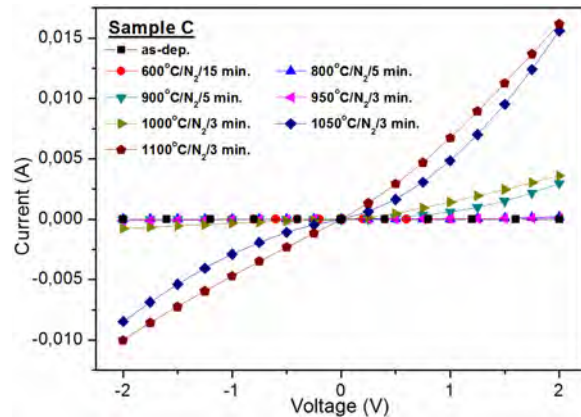
Fig. 4 I-V characteristics measured for a Ni/Si/Ni/Si/n-SiC structure as deposited and after subsequent annealing steps at 600 °C, and then from 950 °C to 1050 °C with a step of 50 °C. The thicknesses of the Ni and Si films were equal to 13.75 nm and 50.5 nm, respectively (sample 'Ni-Si-C' from table 1).

The XRD patterns of the 'Ni-Si-A' sample presented in figure 5 show, that after annealing at 1100 °C the $NiSi_2$ phase crystallizes. As the chemical composition of the deposited stack is not enough for this phase to form, the additional silicon must be thus etched away from the SiC substrate. This claim is supported by RBS depth profiling in figure 6, where it is evident, that although the spectra taken for the 'Ni-Si-A' sample after deposition differ from the spectra taken after annealing at 600 °C and 1050 °C only by the smearing out of the Ni and Si peaks indicating intermixing in the metallisation stack, after annealing at 1100 °C the Si edge for the SiC substrate moves to lower energies, i.e. deeper into the substrate.
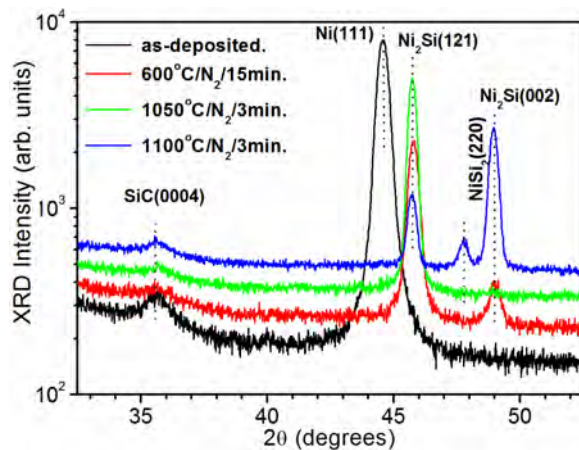

Fig. 5 X-ray diffraction pattern for the sample 'Ni-Si-A' as deposited and after subsequent annealing steps at 600 °C, and then 1050 °C and 1100 °C.
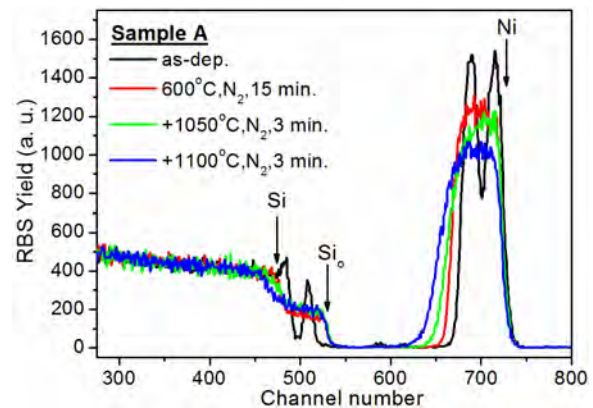
Fig. 6 RBS depth profiles measured for the sample 'Ni-Si-A' after subsequent annealing steps at 600 °C, and then 1050 °C and 1100 °C.

A comparison of the contact surface morphology after annealing at 1050 °C and 1100 °C by means of optical microscopy is shown in figure 7. It is clear, that for the conditions where the $NiSi_2$ phase appears, both in the 'Ni-Si-A' and -B as well as in the 'Ni-Si-C' and -D samples, the morphology becomes very rough which also evidences chemical reactions at the interface with the substrate.
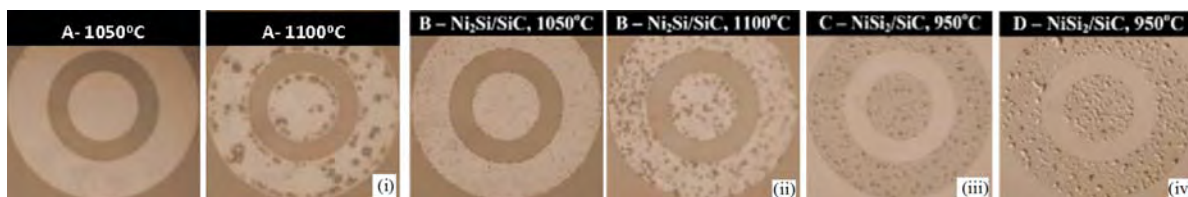
Fig. 7 Optical photographs of contact surface morphologies for the following samples (i) 'Ni-Si-A' after annealing at 1050 °C and 1100 °C, (ii) 'Ni-Si-B' after annealing at 1050 °C and 1100 °C, (iii) 'Ni-Si-C' after annealing at 950 °C, and (iv) 'Ni-Si-D' after annealing at 950 °C.

We may therefore conclude, that the phase Ni_2Si is the one, that leads to ohmic contact formation to n-SiC, where the presence of the $NiSi_2$ phase inhibits the formation of an ohmic contact. A question, that now needs addressing is the explanation of the mechanism of the contact formation in the presence of the Ni_2Si phase. From the XRD patterns presented earlier in figure 5, the presence of single orientation Ni_2Si (121) visible after annealing at 1050 °C can be correlated with the lowest specific contact resistivity determined through cTLM.
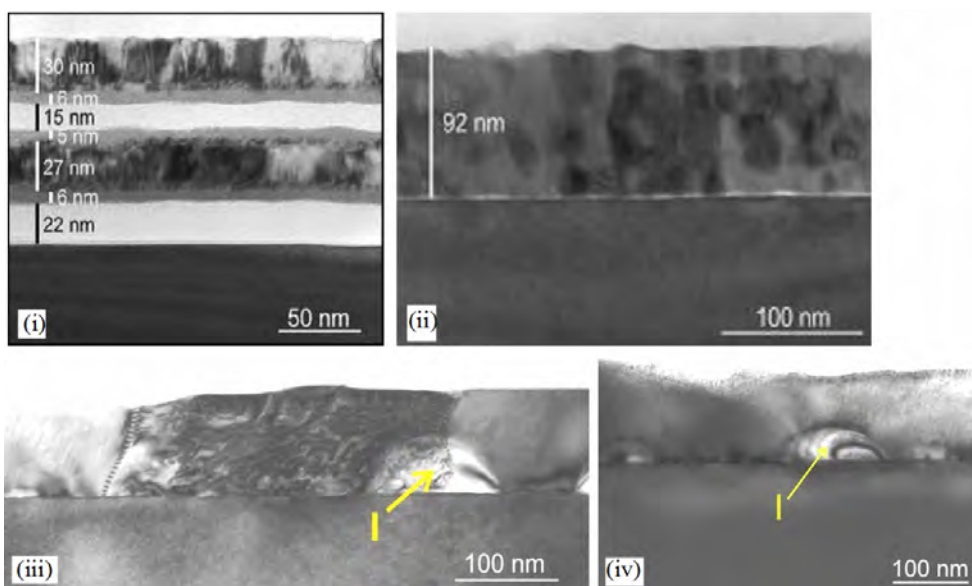

Fig. 8 TEM cross-section micrographs for the sample 'Ni-Si-A' taken (i) after deposition, (ii) after annealing at 600 °C, (iii) after annealing at 1050 °C, and (iv) after annealing at 1100 °C. The 'I' mark voids at grain boundaries.

TEM observations presented in figure 8 lead to the conclusion, that although there are significant structural changes taking place in the metallisation, the interface remains planar after annealing at temperatures as high as 1050 °C. After annealing at 1100 °C, it is clear, that the interface is no longer planar, due to the Si etching evidenced previously. The electron diffraction accompanying these images revealed, that after annealing at 600 °C, traces of Ni_3Si_2 and $Ni_{31}Si_{12}$ phases could be found in the grains, and after annealing at 1050 °C the grains were single crystalline Ni_2Si.

These observations cannot however explain the formation of an ohmic contact, as pure Ni_2Si to SiC junction has the barrier height equal to 1.6 eV as reported for experimental studies, with calculations based on the thermionic emission theory [6]. Therefore we adapted the model proposed by Yu for contacts to n-Si in 1970 [7]. This model takes into account the thermionic emission, field emission and thermionic field emission regimes for current flow across the barrier and allows to determine the specific contact resistivity as a function of the doping concentration for a given barrier height. In the adaptation we changed the values of the relative dielectric constant $\varepsilon_r = 9.66 \cdot \varepsilon_0$, energy gap $E_g = 3.23$ eV and the Richardson constant $A^* = 146$ A·K^{-2}·cm^{-2} to

those of SiC. Furthermore, we changed the electron mass used in the calculations to the electron mass in SiC, $m^* = 0.349 \cdot m_0$, calculated from the electron masses measured by Son et al. [8] using optically detected cyclotron resonance (ODCR). This allowed us to calculate the specific contact resistivities of metal-SiC junctions as a function of doping density of SiC for different barrier heights of the junctions, which is presented in figure 9.
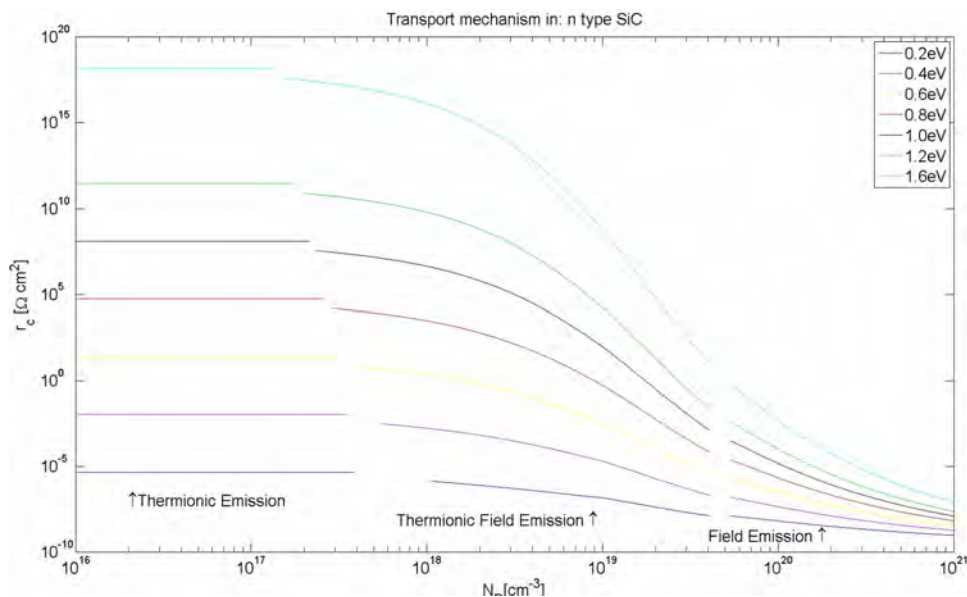

Fig. 9 Calculated specific contact resistivity of a metal/n-SiC contact as a function of semiconductor doping level and barrier height at metal/semiconductor interface based on the modified Yu model described in the text. The areas of different current transport mechanisms are marked in the image.

From this figure it is evident, that in order to have specific contact resistivity of $3.5 \times 10^{-4}\,\Omega \cdot cm^2$ there are two possible solutions: (1) either the doping density in the subcontact region rises to the order of more than $10^{20}\,cm^{-3}$ while keeping the 1.6 eV barrier height or (2) the barrier height is lowered to around 0.3 eV while keeping the $2 \times 10^{17}\,cm^{-3}$ doping density. As we see that in our investigations the interface with SiC is sharp we may assume that no interdiffusion took place, therefore we can discard the first possibility. Therefore what is left is the second solution, i.e. a lowering of the barrier height. Up to this date we cannot explain the exact mechanism of this lowering, however based on the presented characterization data, we claim that there is a reaction at the most intimate Ni_2Si-SiC interface which cannot be evidenced by the present TEM investigations. The work on this subject will continue, however in the next subsection, concerning ohmic contacts to p-SiC, a situation will be described, where the barrier height of the metal/p-SiC junction is lowered by such a reaction at the very intimate interface.

3.2 Al-Ti based ohmic contacts to p-SiC The typical ohmic contact to p-SiC yielding low contact resistivities is a Al/Ti bilayer, with aluminum being the layer directly at the interface to the semiconductor. Pecz et al. [9] studied such a junction using I-V characterization and TEM cross section imaging for a 150 nm Al/30 nm Ti bilayer deposited onto p-SiC with the doping density of $1.6 \times 10^{19}\,cm^{-3}$. After deposition the I-V characteristics were rectifying, but after an annealing at 900 °C for 4 min in a nitrogen flow, the contacts became ohmic, with the specific contact resistivity equal to $4 \times 10^{-4}\,\Omega \cdot cm^2$. The ideal Schottky barrier height of Al/Ti to p-SiC is 1.9 eV directly after deposition as extracted from experimental investigations [10]. From the TEM investigations in the work by Pecz [9], it was shown, that after annealing the Al/Ti bilayer reacts with the substrate to form a Ti_3SiC_2 film directly at the interface and a $TiAl_3$ film on the Ti_3SiC_2. The relatively thick Al layer in the deposited bilayer can be thus thought as promoting the reaction with the substrate. However, the Schottky barrier height for Ti_3SiC_2 is not much lower than for Al/Ti, as it is equal to 1.3 eV as calculated by Gao [11]. If we applied again the model discussed above, but this time substituted electron mass with hole

mass calculated to be $m^* = 1.081 \cdot m_0$ on the basis of measurements performed by Son et al. [12] using ODCR, we would obtain the specific contact resistivity characteristics presented in figure 10.
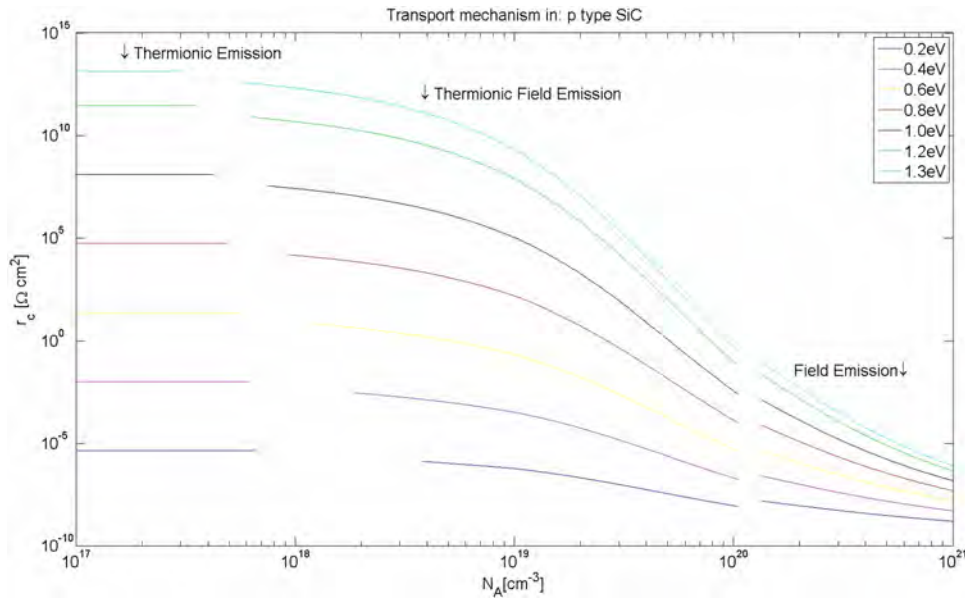

Fig. 10 Calculated specific contact resistivity of a metal/p-SiC contact as a function of semiconductor doping level and barrier height at metal/semiconductor interface based on the modified Yu model described in the text. The areas of different current transport mechanisms are marked in the image.

Similarly to the case of Ni_2Si, to obtain the specific contact resistivity of $4 \times 10^{-4}\,\Omega \cdot cm^2$, either a increase in the doping density or a lowering of the barrier height has to take place. The paper of Wang et al. [13] presents a possible answer to this case using first principle calculations. In figure 5 of the cited paper a high resolution TEM cross section image of the Ti_3SiC_2/SiC junction is presented exhibiting an atomically flat, featureless interface. The starting configuration of the bilayer was 100 nm Ti and 380 nm Al which was annealed at 1000 °C for 2 min in ultra high vacuum. The authors have then calculated the possible atomic configurations and resulting Schottky barrier heights and they show, that a single atomic layer of carbon introduced at the very interface yields the lowest barrier height of the junction, of 0.6 eV. This height is still to large when compared to our simulation results, but it shows, that there are interface reactions which are indistinguishable in high resolution TEM, but may influence the junction barrier height significantly.

4   Ohmic contacts to GaN

Similarly as in the case of SiC, in order to fabricate an ohmic metal-GaN junction one has to deposit the appropriate metallic combination and follow it with annealing. The thermally activated reactions between metals and GaN are very similar to the ones taking place for SiC, only this time for low temperature annealings of Ni, Pd and Pt gallides and nitrogen form, and for the high temperature annealings of refractory metals, nitrides and gallium form. Below follow the applications of different metallisations for ohmic contacts to GaN.

4.1   Ti, Al and N-based ohmic contacts to n-GaN   The metallisation widely recognized as yielding the lowest specific contact resistivity to n-GaN is a Ti/Al bilayer [14], similar to the one deposited in the case of p-SiC, however here titanium, not aluminum, is the layer at the interface with the semiconductor. The specific contact resistivity of such a junction lies within 10^{-5}-$10^{-7}\,\Omega \cdot cm^2$ for n-GaN doped to 10^{17}-$10^{18}\,cm^{-3}$. The mechanism of ohmic contact formation lies in this case in the outdiffusion of nitrogen from the GaN substrate in the vicinity of the interface and the creation of a TiN layer from the Ti. Taking into account, that TiN deposited on GaN does not form an ohmic contact, it is believed, that nitrogen vacancies acting as shallow

donors in GaN, create a subcontact n^{++} region, diminishing the Schottky barrier width significantly and enabling carrier transport through the barrier by tunneling [14]. However the role of nitrogen vacancies in n-GaN is still the subject of debate [15]. The Al acts as a promoter of the reaction, similarly to the Ti_3SiC_2/SiC case described above.

This metallisation is however not resistant to elevated temperatures of the order of 600 °C [16] at which the ohmic character of the junction breaks down as Al-phases form at the interface. In order to have ohmic contacts that would be stable at elevated temperatures it is possible to substitute the Ti/Al metallisation for a similar one. One approach could be to replace the Al with a refractory metal nitride, such as TiN [17]. The contact would then again form via nitrogen outdiffusion from GaN, however as TiN is highly resistive to elevated temperatures, the thermal stability of such a contact would highly improve, while maintaining the low specific contact resistivity, comparable to that of the Ti/Al-based one. In the cited work the specific contact resistivity did not change after 5 days of annealing in an evacuated quartz tube at 600 °C.

Another approach would be to substitute the Ti/Al system by a Ti/Al/TiN system that would lead to the formation of the MAX phase Ti_2AlN. The MAX phases are a group of ternary compounds of the chemical formula $M_{n+1}AX_n$, where M – refractory metal, A – group IVA or VA element and X - carbon or nitrogen, which were first described by Novotny [18] and in recent years the group of Barsoum [19] studied them extensively. Due to their nanocomposite laminar structure they exhibit both ceramic (high temperature resistance, resistance to oxidation) and metallic (high electric and thermal conductivity) properties. It can be easily seen, that the Ti_3SiC_2 described previously is also a member of this group. Based on the idea that Ti_2AlN would be more stable thermally than Ti/Al while maintaining similar specific contact resistivity, we performed an experiment aimed at studying the phase formation in a Ti/Al/TiN multilayer [20]. The thicknesses of the Ti/Al/TiN films were set in such a way, that the atomic ratios in the stack would represent the Ti_2AlN chemical composition (i.e. 16 nm for Ti and Al and 20 nm for TiN). However, after annealing at 600 °C in Ar, we observed the formation of Ti_2AlN only at the interface with the GaN and not in the whole stack. A promising specific contact resistivity of the order of 10^{-4} $\Omega \cdot cm^2$ was obtained on n-GaN doped at 10^{16} cm^{-3}. No thermal stability tests have been performed yet

4.2 NiAu and PdAu ohmic contacts to p-GaN   Au-based metallizations such as NiAu or PdAu have been proven to give low resistivity ohmic contacts to p-GaN ($r_c \sim 10^{-4}$ $\Omega \cdot cm^2$). In particular, the low resistivity and crystalline ordering of metallization (epitaxial NiO–Au composite in the case of the first system or single-crystalline PdAu layer in the latter) with an abrupt interface to GaN were attributed to the substantial elimination of oxidation layers at the interface during thermal annealing [21,22].

5   Thermal stability of the contacts via the application of diffusion barriers

As it was mentioned before, elevated temperatures and corrosive environments can lead to a significant degradation of ohmic contacts and their performance, as we have shown on the example of the Ni_2Si ohmic contacts to n-SiC that have been covered with 150 nm of Au mounting layer [23,24]. When exposed to annealing in air at 400 °C, the contacts loose their ohmic character. This is evidenced in figure 11 where the I-V characteristics of such contacts are presented for the 'as formed' state and for different subsequent annealing of 50 and 150 h. One can easily see, that after the first annealing the contact resistivity rises and after the prolonged ageing the I-V character changes to a non-ohmic one.

Based on the XRD patterns presented in figure 12 we see that at the first annealing step the Au_xSi_{1-x} phase grows with a massive Ni_2Si decomposition and the appearance of pure Ni and Au_xNi_{1-x} at higher anneal times. We may correlate these changes with the SEM images of the surface in figure 13 where after the first annealing step small crystallites appear on the surface of the sample, which may be the Au_xSi_{1-x} phases and after the second step significant changes to the surface appear, possibly due to Ni_2Si decomposition.

In order to elevate the temperatures of contact stability or to encapsulate the contacts against corrosive work environments, diffusion barriers may be introduced into the contact stack, below the Au mounting layer. There can be different mechanisms in which the barrier works, most notably preventing the intermixing of the

active contact metallisation with the Au layer and environmental oxygen, but also impeding reactions in the contact metallisation itself – an effect which is not yet well understood. As far as diffusion blocking is concerned, the fast diffusion routes in the films are grain boundaries and defects. Thus, in order to block the diffusion one should eliminate the grain boundaries or introduce diffusion blocking interfaces between the films, depending on their microstructure. The possible microstructures of diffusion barriers with the respective mechanisms of diffusion blocking are put together in table 2. It can seem, that conductive amorphous or monocrystalline films would be the best choices for applications in diffusion barriers due to the simplicity of the solution. However, one has to remember that the formation of monocrystalline conductive films most often requires the application of elevated temperatures, which would adversely influence the contact. Furthermore, the introduction of a second film may appear as an unnecessary complication but is often beneficial as the interface blocking mechanism is added. In this mechanism even polycrystalline thin films of different crystalline structures can impede interdiffusion.
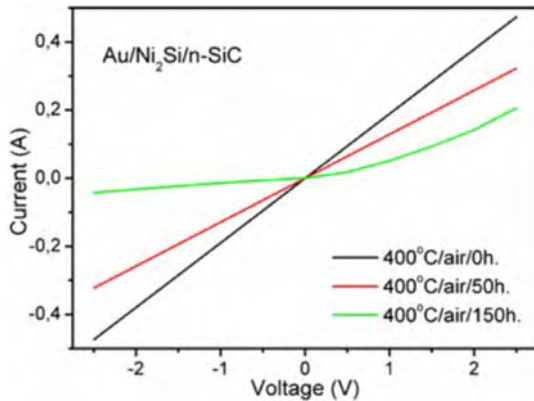

Fig. 11 I-V characteristics of Au/Ni$_2$Si/n-SiC structures after ohmic contact formation at 1050 °C and subsequent ageing in air at 400 °C. The thicknesses of the films were: 150 nm and 100 nm for Au and Ni$_2$Si, respectively.
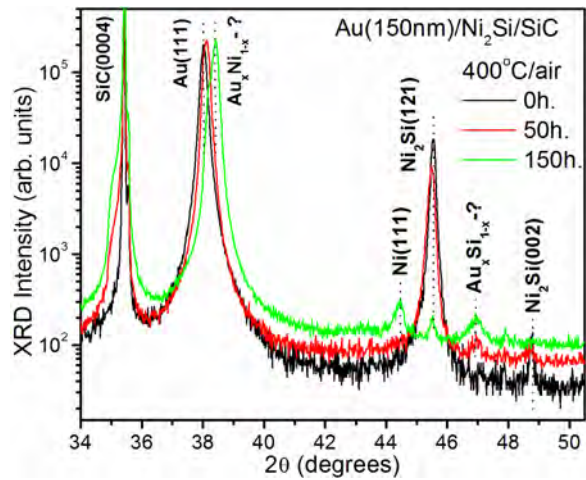

Fig. 12 XRD patterns for the Au/Ni$_2$Si/n-SiC structures after ohmic contact formation at 1050 °C and subsequent ageing in air at 400 °C. The thicknesses of the films were: 150 nm and 100 nm for Au and Ni$_2$Si, respectively.
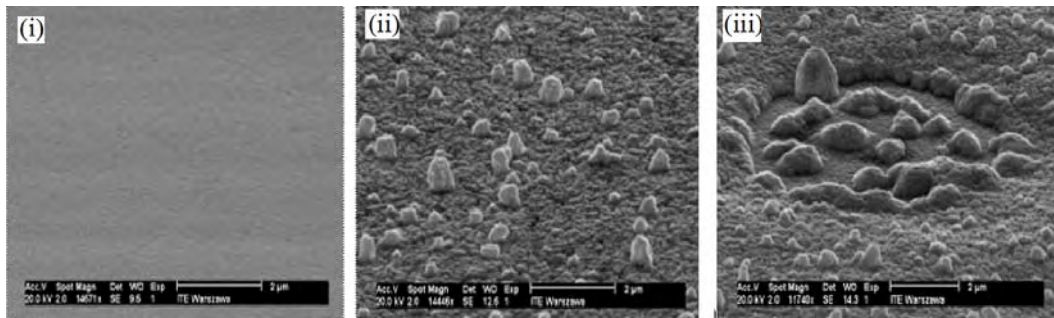

Fig. 13 SEM plan-view images of the Au/Ni$_2$Si/n-SiC structures after ohmic contact formation at 1050 °C (i) and subsequent ageing in air at 400 °C for 50 h (ii) and 150 h (iii). The thicknesses of the films were: 150 nm and 100 nm for Au and Ni$_2$Si, respectively. Image magnification 12000.

We have applied a 120 nm amorphous Ta$_{0.34}$Si$_{0.25}$N$_{0.41}$ diffusion barrier in between the Ni$_2$Si and the Au layers in the contact stack to improve the thermal stability. The composition of the barrier was optimized in order to obtain the lowest contact resistivity and stress on the substrates. After the annealing tests, the ohmic behavior was found to be kept even after annealing for 150 h at 400 °C in air. The specific contact resistivity rose by a

factor of 2 after annealing at 50 h and then did not change after the next annealing step. This drop is attributed to the formation of minority Ni_2Si (001) phase as evidenced from XRD patterns presented in figure 14.

Table 2 Layer systems of diffusion barriers.

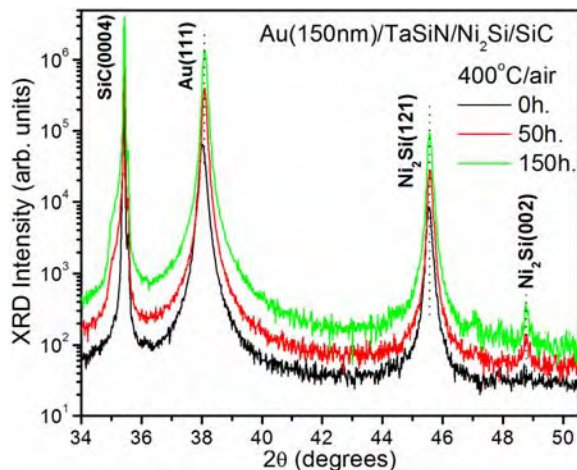| Layer system	Diffusion blocking through
Amorphous thin film	No grain boundaries
Monocrystalline thin film	No grain boundaries
Multilayer amorphous thin films	No grain boundaries + interface blocking
Multilayer polycrystalline thin films of different crystalline structures	Interface blocking

Fig. 14 XRD patterns for the $Au/TaSiN/Ni_2Si/n$-SiC structures after ohmic contact formation at 1050 °C and subsequent ageing in air at 400 °C. The thicknesses of the films were: 150 nm, 120 nm and 100 nm for Au and TaSiN and Ni_2Si, respectively.

It is clear, that compared to the situation without the TaSiN barrier, the Ni_2Si does not decompose and the microcrystalline structure does not change much. The final evidence of the efficiency of the TaSiN barrier is shown in figure 15 where the SEM plan-view images before and after ageing tests show a featureless surface in both cases. This Ta-Si-N barrier, among with similar Ti-Si-N and Ti-W-N has also been tested on ohmic contacts to GaN, in particular p-GaN [25].
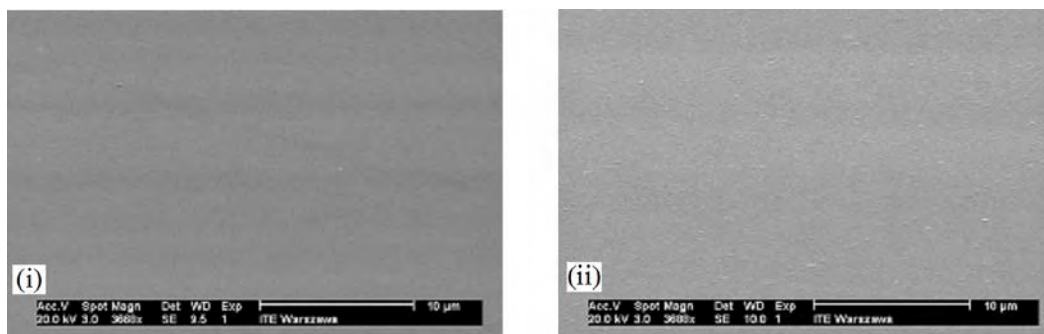
Fig. 15 SEM plan-view images for the $Au/TaSiN/Ni_2Si/n$-SiC structures after ohmic contact formation at 1050 °C (i) and subsequent ageing in air at 400 °C for 150 h (ii). The thicknesses of the films were: 150 nm, 120 nm and 100 nm for Au and TaSiN and Ni_2Si, respectively. Image magnification is 4000.

A good example of the stability of polycrystalline multilayers would be the ZrB_2/ZrN layer system. The default crystalline structures of the materials are different, being hexagonal for ZrB_2 and cubic for ZrN. If a bi- or multilayer of these films is deposited under such process conditions, that both ZrB_2 and ZrN grow microscopically amorphous, then upon annealing at temperatures high enough to promote the crystallization, the resulting thin film stack will consist of intertwined cubic and hexagonal thin films, between which no easy diffusion is possible due to the mismatch of the crystalline lattice geometries. We found that the interfaces

between ZrB_2 and ZrN films in such stacks remain flat after the crystallization upon annealing [26]. According to these studies, the stability of such systems was: 1000 °C for 30 s in a nitrogen flow for the bilayer and 800 °C for 30 min in an nitrogen flow for a multilayer composed of 13 bilayers, respectively.

6 Conclusion

In the technology of ohmic contacts to wide band gap semiconductors such as GaN and SiC interfacial reactions are very often important, even at a very intimate interface, which cannot be resolved using even high resolution TEM. Therefore the modelling of junction properties can be an important tool in the determination of contact properties and explanation of the contact forming mechanisms. Nevertheless, still a number of fundamental questions exist concerning the issue, such as the exact determination of the role of carbon at the interface in the case of Ni_2Si/n-SiC contacts, or of aluminium in the formation of Ti_3SiC_2 in the AlTi/p-SiC contacts. As the issue of thermal stability of the metallisations is a significant issue for wide band gap semiconductors due to the harsh work environments, we showed that it was beneficial to introduce a diffusion barrier into the metallisation stack. The design of the barriers is a complex problem, that has to take into account the temperature, stability time and atmosphere of work for the future device. Refractory metal nitrides, carbides, borides and ternary compounds were shown to be promising materials for such applications.

References

[1]   Y.-M. Lin, C. Dimitrakopoulos, K. A. Jenkins, D. B. Farmer, H.-Y. Chiu, A. Grill, and Ph. Avouris, Science **327**, 662 (2010).

[2]   M. V. Sullivan and J. H. Eigler, J. Electrochem. Soc. **104**, 226 (1957).

[3]   Ts. Marinova, A. Kakanakova-Georgieva, V. Krastev, R. Kakanakov, M. Neshev, L. Kassamakova, O. Noblanc, C. Arnodo, S. Cassette, C. Brylinski, B. Pecz, G. Radnoczi, and G. Vincze, Mater. Sci. Eng. B **46**, 223 (1997).

[4]   A. V. Kuchuk, V. P. Kladko, A. Piotrowska, R. Ratajczak, and R. Jakiela, Mater. Sci. Forum **615-617**, 573 (2009).

[5]   A. V. Kuchuk, V. Kladko, M. Guziewicz, A. Piotrowska, R. Minikayev, A. Stonert, and R. Ratajczak, J. Phys. Conf. Ser. **100**, 042003 (2008).

[6]   F. Roccaforte, F. La Via, V. Raineri, R. Pierobon, and E. Zanoni, J. Appl. Phys. **93**, 9137 (2003).

[7]   A. Yu, Solid State Electron. **13**, 239 (1970).

[8]   T. Son, W. M. Chen, O. Kordina, A. O. Konstantinov B. Monemar, and E. Janzén, Appl. Phys. Lett. **65**, 3209 (1995).

[9]   B. Pécz, L. Tóth, M. A. di Forte-Poisson, and J. Vacas, Appl. Surf. Sci. **206**, 8 (2003).

[10]   S.-K. Lee, C.-M. Zetterling, and M. Osling, J. Electron. Mater. **30**, 242 (2001).

[11]   M. Gao, S. Tsukimoto, S. H. Goss, S. P. Tumakha, T. Onishi, M. Murakami, and L. J. Brillson, J. Electron. Mater. **36**, 4 (2007).

[12]   N. T. Son, P. N. Hai, W. M. Chen, C. Hallin, B. Monemar, and E. Janzén, Phys. Rev. B **61**, R10544 (2000).

[13]   Z. Wang, S. Tsukimoto, M. Saito, K. Ito, M. Murakami, and Y. Ikuhara, Phys. Rev. B **80**, 245303 (2009).

[14]   M. E. Lin, Z. Ma, F. Y. Huang, Z. F. Fan, L.A. Allen, and H. Morkoc, Appl. Phys. Lett. **64**, 1003 (1994).

[15]   D. C. Look, G. C. Farlow, P. J. Drevinsky, D .F. Bliss, and J. R. Sizelove, Appl. Phys. Lett. **83**, 3525 (2003).

[16]   B. P. Luther, S. E. Mohney, J. M. DeLucca, and R. F. Karlicek Jr., J. Electron. Mater. **27**, 1407 (1998).

[17]   E. Kamińska, A. Piotrowska, M. Guziewicz, S. Kasjaniuk, A. Barcz, E. Dynowska, M. D. Bremser, O. H. Nam, and R. F. Davis, Mat. Res. Soc. Symp. Proc. **449**, 1055 (1996).

[18]   H. Novotny, Prog. Solid State Chem. **2**, 27 (1970).

[19]   M. W. Barsoum, Prog. Solid State Chem. **28**, 201 (2000).

[20]   M. A. Borysiewicz, E. Kamińska, A. Piotrowska, I. Pasternak, R. Jakieła, and E. Dynowska, Acta Phys. Pol. A **114**, 963 (2008).

[21]   J. Narayan, H. Wang, T.-H. Oh, H. K. Choi, and J. C. C. Fan, Appl. Phys. Lett. **81**, 3978 (2002).

[22]   C. Kim, J. Jang, J. Shin, J.-W. Choi, J.-H. Seo, W. Kim, J. Park, J. O. Seo, S.-J. Leem, B. H. Seung, K.-B. Lee, and Y. J. Park, Phys. Rev. B **64**, 113302 (2001).

[23] A. V. Kuchuk, M. Guziewicz, R. Ratajczak, M. Wzorek, V. P. Kladko, and A. Piotrowska, Microelectron. Eng. **85**, 2142 (2008).

[24] A. V. Kuchuk, M. Guziewicz, R. Ratajczak, M. Wzorek, V. P. Kladko, and A. Piotrowska, Mater. Sci. Eng. B **165**, 38 (2009).

[25] A. Piotrowska, E. Kaminska, M. Guziewicz, E. Dynowska, A. Stonert, A. Turos, S. Figge, R. Kroger, and D. Hommel, Mater. Res. Soc. Symp. Proc. **892**, 0892-FF14-05.1 (2006).

[26] E. Kaminska, K. Golaszewska, A. Piotrowska, A. Kuchuk, R. Kruszka, E. Papis, R. Szeloch, P. Janus, T. Gotszalk, and A. Barcz, phys. stat. sol. (c) **1**, 219 (2004).